Follow us @BoneJointRes

Freely available online OPEN ACCESS

BJR

BIOMECHANICS

Biomechanical effect of anatomical tibial component design on load distribution of medial proximal tibial bone in total knee arthroplasty

FINITE ELEMENT ANALYSIS INDICATING ANATOMICAL DESIGN PREVENTS STRESS-SHIELDING

B. W. Cho,
K-T. Kang,
H. M. Kwon,
W-S. Lee,
I. H. Yang,
J. H. Nam,
Y-G. Koh,
K. K. Park

From Gangnam Severance Hospital, Yonsei University College of Medicine, Seoul, South Korea

Aims
This study aimed to identify the effect of anatomical tibial component (ATC) design on load distribution in the periprosthetic tibial bone of Koreans using finite element analysis (FEA).

Methods
3D finite element models of 30 tibiae in Korean women were created. A symmetric tibial component (STC, NexGen LPS-Flex) and an ATC (Persona) were used in surgical simulation. We compared the FEA measurements (von Mises stress and principal strains) around the stem tip and in the medial half of the proximal tibial bone, as well as the distance from the distal stem tip to the shortest anteromedial cortical bone. Correlations between this distance and FEA measurements were then analyzed.

Results
The distance from the distal stem tip to the shortest cortical bone showed no statistically significant difference between implants. However, the peak von Mises stress around the distal stem tip was higher with STC than with ATC. In the medial half of the proximal tibial bone: 1) the mean von Mises stress, maximum principal strain, and minimum principal strain were higher with ATC; 2) ATC showed a positive correlation between the distance and mean von Mises stress; 3) ATC showed a negative correlation between the distance and mean minimum principal strain; and 4) STC showed no correlation between the distance and mean measurements.

Conclusion
Implant design affects the load distribution on the periprosthetic tibial bone, and ATC can be more advantageous in preventing stress-shielding than STC. However, under certain circumstances with short distances, the advantage of ATC may be offset.

Cite this article: *Bone Joint Res* 2022;11(5):252–259.

Keywords: Total knee arthroplasty, Finite element analysis, Anatomical tibial component, Stress-shielding, Medial proximal tibial bone loss

Article focus
- This study investigated how the implant design of the tibial component affects the periprosthetic load distribution on knees.

Key messages
- The implant design of anatomical tibial component (ATC), including the medialized stem and the anatomical shape of the baseplate, affects the load distribution on the periprosthetic tibial bone.

Correspondence should be sent to Kwan Kyu Park; email: kkpark@yuhs.ac

doi: 10.1302/2046-3758.115.BJR-2021-0537.R1

Bone Joint Res 2022;11(5):252–259.

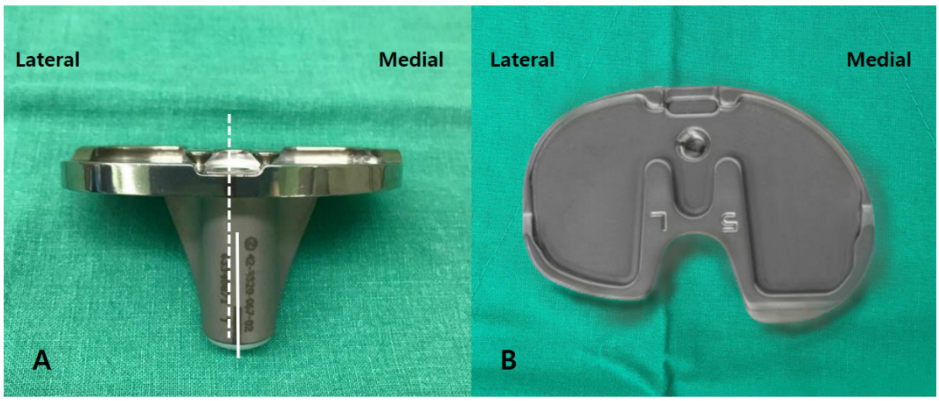

Fig. 1

a) Medialized stem of anatomical tibial component (ATC). b) Asymmetric baseplate of ATC.

- The ATC transmits more load to the medial proximal tibial bone compared to a symmetric tibial component.
- With an ATC, the shorter the distance between the stem and the anteromedial cortical bone, the less load is applied to the medial proximal tibial bone.

Strengths and limitations

- A total of 30 finite element models were used to reflect the anatomical characteristics of Korean women, which enabled statistical analysis for data interpretation.
- Since it is not clear whether the difference of load distribution on the periprosthetic tibial bone is directly related to bone resorption, further study is needed.

Introduction

Total knee arthroplasty (TKA) shows excellent results in the treatment of end-stage knee osteoarthritis.[1] With increased life span after TKA, interest in the longevity of artificial joints has also increased, and various devices are being developed accordingly. Recently, an anatomical tibial component (ATC) designed to enhance clinical outcomes has been introduced by Zimmer Biomet (USA). This implant comprises a medialized stem (Figure 1a) and an anatomically shaped baseplate (Figure 1b), similar to the human tibia. Although this design is used worldwide, certain races and circumstances may show variations that differ from the manufacturer's expectations.

The tibial canal is biased medially in Caucasians;[2] the ATC was designed to achieve optimal alignment with a medialized stem. However, in Asians, the tibial canal is biased anterolaterally from the centre of the tibial plateau,[3] such that a medially offset stem can induce mismatched alignment,[4] causing stress-shielding and bone loss.[5] According to previous literature, there should be less bone loss with an ATC with a shorter stem,[6,7] thinner baseplate,[8] and more tibial plateau coverage,[9] relative to conventional implants. Cho et al[5] reported that an ATC is more likely to induce medial tibial bone loss than a symmetric tibial component (STC) due to stress-shielding in Korean patients. Regarding this matter, they suggested that inefficient stress transfer due to a medialized stem may be one of the causes.[5] However, due to the inherent limitations of their retrospective observational study, a clear mechanism has not been identified.

In clinical practice, controlling factors that affect stress-shielding of the bone around an implant is almost impossible. Therefore, finite element analysis (FEA) has been used in analyzing mechanical stimuli alterations according to the implant design, material, and surgical methods that affect stress-shielding in total joint replacement,[10,11] especially in TKA. Park et al[12] reported the association of periprosthetic tibial bone resorption with tibial component material, and Zhang et al[13] reported that the material and alignment of tibial component had a significant effect on the stress-shielding of the proximal tibia. In addition, Au et al[14] reported that the contribution of loading condition had an important effect on the stress-shielding near the tibial component. However, to our knowledge, there are no FEA studies that analyzed the effect of implant design by controlling other factors.

The present study aimed to identify the effect of ATC design on load distribution in the proximal tibiae using FEA. We hypothesized that an ATC with a medialized stem will have higher stress between the stem distal tip and medial cortical bone compared to an STC, thereby reducing the load on the proximal tibial bone.

Methods

Data collection. With approval from our institutional review board, 30 patients undergoing TKA using an ATC (Persona, Zimmer Biomet) were retrospectively enrolled.

Table I. Patient demographic data.

Characteristic	Value
Female sex, %	100
Right knee, %	50
Mean age, yrs (SD; range)	71.2 (5.9; 59 to 79)
Mean height, cm (SD; range)	154.9 (4.7; 149.1 to 165.0)
Mean BMI, kg/m² (SD; range)	27.3 (3.4; 22.2 to 33.2)

SD, standard deviation.

Table II. Specifications of both implants.

Variable	ATC (Persona D)	STC (NexGen 3)
Baseplate medio-lateral length	67.1 mm	66.5 mm
Baseplate thickness	3.68 mm	4.18 mm
Stem length	31.4 mm	39.7 mm
Material	Ti6Al4V	Ti6Al4V
Sagittal angle between stem axis and baseplate	5°	7°
Stem diameter at distal tip (metal part)	14.2 mm	14.48 mm
Distance from anterior border to stem centre at baseplate	13.05 mm	12.3 mm

ATC, anatomical tibial component; STC, symmetric tibial component.

Since the stem was 1 to 4 mm medialized depending on the size of the tibial component, only patients with size D were enrolled.

Patient demographic data are shown in Table I. All patients were female, and 15/30 knees (50%) were right-sided. The mean age was 71.2 years (standard deviation (SD); 59 to 79), the mean height was 154.9 cm (SD 4.7; 149.1 to 165.0), and the mean BMI was 27.3 kg/m² (SD 3.4; 22.2 to 33.2).

Finite element model and surgical simulation. Preoperative CT (GE Discovery CT 750 HD, GE Medical Systems; tube voltage, 120 kV; tube current, 185 mAs/slice; pitch factor, 0.426; matrix, 512 × 512; reconstructive thickness, 0.625 mm) Digital Imaging and Communications in Medicine (DICOM; National Electrical Manufacturers Association, USA) data were imported into Mimics software (version 21.0; Materialize, Belgium). A well-trained technician segmented the areas of interest by applying manual and automated thresholding techniques to the raw DICOM data. The segmented masks of DICOM data were converted to STL format. The wrapping technique was applied on the STL. The gap closing distance was 1 mm. After wrapping, smoothing algorithm was applied on the STL with smooth factor 0.1, and the iteration was 5. The 3D STL model was converted to the Initial Graphics Exchange Specification (IGES) format to create the mesh element.

3D finite element models (FEMs) were created using modified tetrahedral ten-node elements with ABAQUS software 6.11 (ABAQUS, USA). It was assumed that the tibial component and tibial bone were completely fixed. The isotropic material values (Young's modulus of elasticity and Poisson's ratio v) were as follows: cancellous bone (0.7 GPa, 0.30), cortical bone (17 GPa, 0.30), cement (2.2 GPa, 0.46), and Ti6Al4V (110 GPa, 0.30).[15] The thickness of the cortical bone and cement was set to 2 mm. Cementation was applied between the baseplate and the proximal tibia.[16] The load was set to approximately 2,000 N, considering that thrice the load is applied in the late stance phase when a 70 kg adult walks. The load was divided into 7:3 ratios on the medial and lateral condyles, respectively.[15,17,18] A mesh convergence analysis of maximum displacement in the FEMs was assessed, similar to a previous study.[19] The convergence rate of maximum displacement was < 0.1% in all models. The number of elements was as follows: tibial plate, 151,902; cement, 48,654; cortical bone, 293,444; and cancellous bone, 425,015.

The surgical simulation was performed as follows. The tibial shaft was defined as a line connecting the centre between the tibial spines and the centre of a sphere fitted to the talocrural joint. The proximal tibia was cut perpendicular to the tibial shaft with a posterior slope of 3°; the cutting level was set to 8 mm from the highest side of the tibial plateau (all lateral condyles in this study). During implant insertion, the anteroposterior position was aligned with the anterior border, and the mediolateral position was placed in the middle.

The rotation of tibial components was aligned to the line between the centre of posterior cruciate ligament footprint and medial third of the tibial tubercle. A STC (NexGen LPS-Flex size 3) and ATC (Persona size D) from a single manufacturer (Zimmer Biomet) were used. The specifications of these implants are presented in Table II.

Finite element model measurements. When each implant was inserted and load applied, the stress concentration and the risk of stress-shielding around the distal stem tip and in the medial half of 5 mm thick proximal tibial bone were evaluated (Figure 2).[15,20–22] To evaluate the stress concentration around the stem distal tip and the medial half of 5 mm thick proximal tibial bone, the peak von Mises stress among the cancellous bone elements was measured. To evaluate the risk of stress-shielding to the tibial cutting plane, the mean von Mises stress and mean principal strains of the medial half of 5 mm thick proximal tibial cancellous bone were measured.

When each implant was inserted, the distance from the distal stem tip to the shortest anteromedial cortical bone was measured and analyzed. The distance was measured on a plane perpendicular to the stem axis passing through the most distal part (Figure 3). To evaluate intra- and interobserver reliability of distance measurements, the models were evaluated by two orthopaedic surgeons (BWC, YGK) at four-week intervals.

Statistical analysis. A paired *t*-test was performed to compare the differences in stress, strain, and distance according to implant type. Pearson correlation analysis

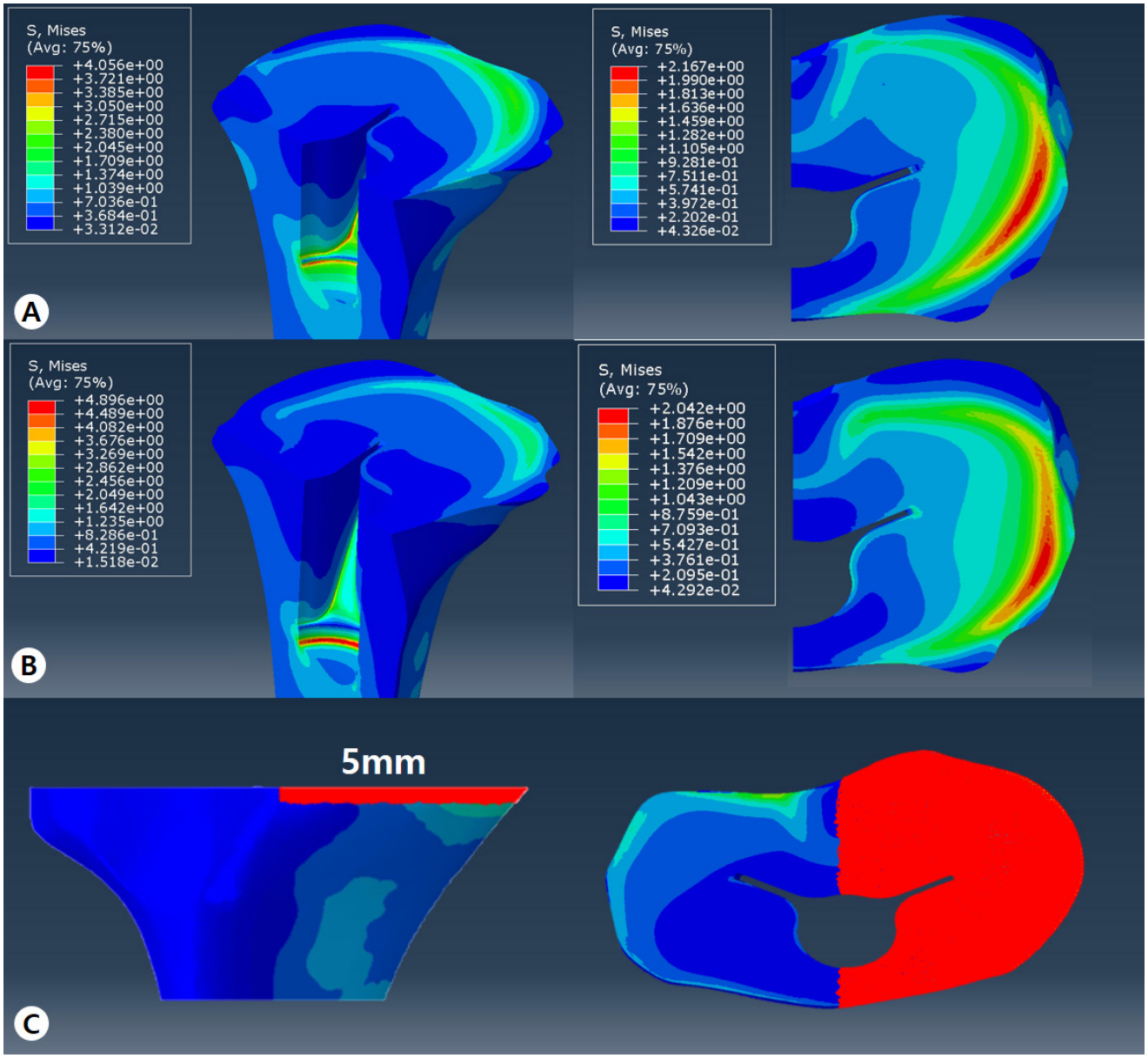

Fig. 2

a) Von Mises stress plot of anatomical tibial component for cancellous bone around the distal stem tip and the medial half of 5 mm thick proximal tibial bone.
b) Von Mises stress plot of symmetric tibial component for cancellous bone around the distal stem tip, and the medial half of 5 mm thick proximal tibial bone.
c) Region of interest in medial proximal tibia.

was performed to evaluate the relationship between distance and FEA measurements. Statistical analysis was performed using SPSS statistical software (version 25.0, IBM, USA). Statistical significance was set at $p < 0.05$. The intra- and interobserver reliabilities of the measurements were assessed using intraclass correlation coefficients.

Results

Table III shows the stress, strain, and distance measurements when ATC and STC were inserted. The mean distance from the distal stem tip of the two implants to the shortest cortical bone showed no statistically significant difference (ATC 3.91 mm (SD 1.07) and STC 3.91 mm (SD 1.18), $p = 0.979$, paired *t*-test). However, the mean maximum von Mises stress near the distal stem tip was higher with STC than with ATC (5.52 MPa (SD 0.64) and 4.41 MPa (SD 0.39), $p < 0.001$, paired *t*-test). In the medial half of the proximal tibial bone, the peak von Mises stress showed no statistical difference between the two implants (ATC 2.66 MPa (SD 0.64) and STC 2.71 MPa (SD 0.61), $p = 0.247$, paired *t*-test); but the mean von Mises stress, maximum principal strain, and minimum principal strain were higher with ATC (ATC 0.453 MPa (SD 0.021) and STC 0.404 MPa (SD 0.017), $p < 0.001$; ATC

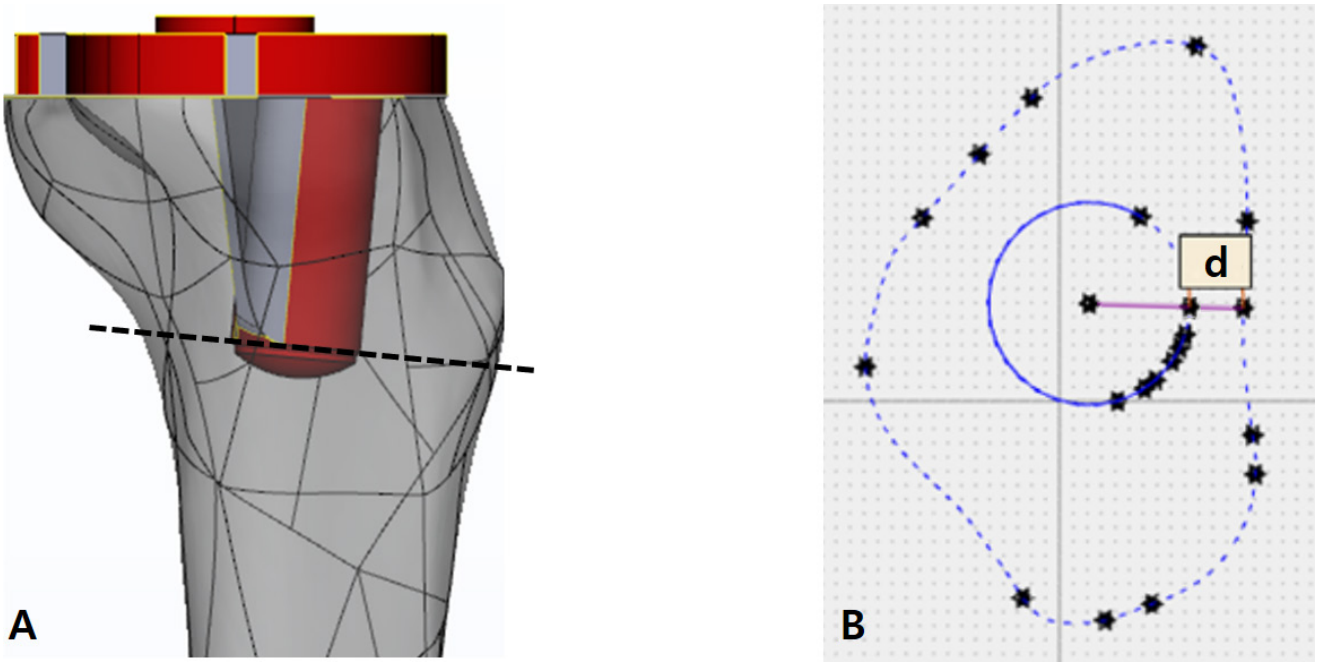

Fig. 3

a) Surgical simulations of anatomical tibial component. b) The plane perpendicular to the stem axis at the most distal end. d = the shortest distance between distal stem tip and anteromedial cortical bone.

Table III. Results of paired *t*-test analysis between anatomical tibial component and symmetric tibial component.

Variable	ATC	STC	p-value
Mean distance between stem tip and cortical bone, mm (SD; range)	3.91 (1.07; 1.59 to 6.05)	3.91 (1.18; 1.13 to 5.61)	0.979
Around stem tip area			
Mean peak von Mises stress, MPa (SD; range)	4.41 (0.39; 3.70 to 5.47)	5.52 (0.64; 4.18 to 7.49)	< 0.001
Medial half of proximal tibial bone			
Mean peak von Mises stress, MPa (SD; range)	2.66 (0.64; 1.83 to 4.39)	2.71 (0.61; 1.66 to 3.87)	0.247
Mean von Mises stress, MPa (SD; range)	0.453 (0.021; 0.405 to 0.487)	0.404 (0.017; 0.373 to 0.428)	< 0.001
Mean maximum principal strain, μstrain (SD; range)	305 (14; 282 to 335)	272 (9; 253 to 290)	< 0.001
Mean minimum principal strain, μstrain (SD; range)*	-622 (32; -674 to -546)	-553 (29; -596 to -550)	< 0.001

*Minimum principal strain was expressed as a negative value.
ATC, anatomical tibial component; STC, symmetric tibial component; SD, standard deviation.

305 μstrain (SD 14) and STC 272 μstrain (SD 9), p < 0.001; ATC -622 μstrain (SD 32) and STC -553 μstrain (SD 29), p < 0.001, all paired *t*-test).

Table IV shows the correlation between the distance from the distal stem tip to the cortical bone and FEA measurements. ATC and STC showed a negative correlation between this distance and peak stress around the distal stem tip (ATC r = –0.459, p = 0.014; STC r = –0.536, p = 0.003, Pearson correlation analysis). In the medial half of the proximal tibial bone, ATC showed a positive correlation of distance with the mean von Mises stress (r = 0.434, p = 0.021, Pearson correlation analysis) and a negative correlation of distance with the mean minimal principal strain (r = –0.417, p = 0.027, Pearson correlation analysis). STC showed no correlation between distance and mean values in the medial half of the proximal tibial bone.

The intra- and interobserver reliabilities for the distance measurement were 0.975 and 0.872, respectively.

Discussion

The most important finding of the present study is that the implant design, including medialized stem and the anatomical shape of the baseplate, affects the load distribution on the periprosthetic tibial bone. Although the stem of ATC was medialized, the distance to the shortest cortical bone did not differ from that of STC due to the length and sagittal angle of the stem. When the same body weight was applied to the FEM, ATC had a lower peak stress on the distal stem tip, and higher mean strain and stress on the medial half of the proximal tibial bone compared to STC, which is more advantageous in preventing stress-shielding. However, the effect of distance change on load distribution differed for each

Table IV. Results of Pearson correlation analysis between the distance from distal stem tip to cortical bone and stress/strain measurements.

Correlation with distance	ATC		STC	
	r	p-value	r	p-value
Around stem tip area				
Peak von Mises stress	-0.459	0.014	-0.536	0.003
Medial half of proximal tibial bone				
Peak von Mises stress	0.044	0.825	0.166	0.400
Mean von Mises stress	0.434	0.021	0.293	0.130
Mean maximum principal strain	0.254	0.191	0.140	0.479
Mean minimum principal strain	-0.417	0.027	-0.291	0.133

ATC, anatomical tibial component; STC, symmetric tibial component.

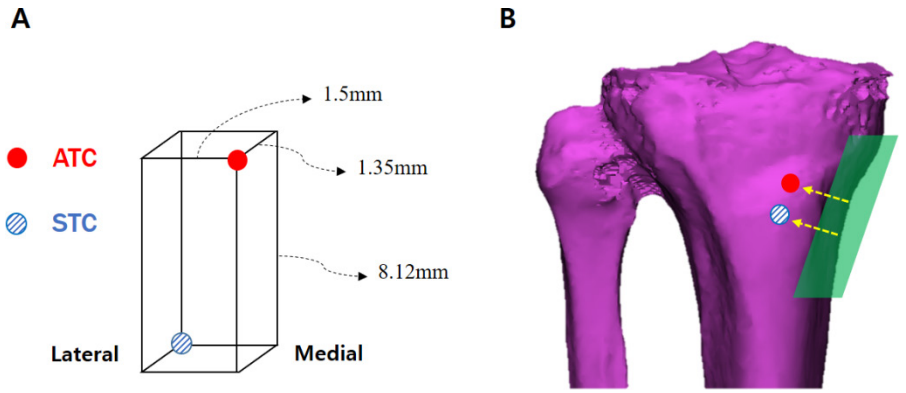

Fig. 4

a) Schematic composite image showing the positional relationship of the central point of the stem tip metal portion when anatomical tibial component (ATC) and symmetric tibial component (STC) are inserted with the same reference. b) Due to the oblique orientation of anteromedial cortical bone, there is no statistical difference in the shortest distance between two implants.

implant, suggesting that the advantage of ATC may be offset under certain circumstances.

There are two considerations to take into account before interpreting our results. First, our study did not directly predict stress-shielding through a well-established method as in the previous literature, but compared the load given to a specific region of interest between implants through statistical values of 30 models. Since most of the FEA studies use one or a limited number of models, they try to predict bone resorption based on specific thresholds, but these values vary from study to study.[23-25] This is because bones respond differently to load depending on race, sex, age, and situations. Therefore, our study obtained the mean measurements of 30 Korean women, and tried to judge the possibility of bone resorption through statistical comparison, not based on a specific threshold. However, since it is not yet known whether the difference in the mean measurements of the elements causes a difference in actual bone resorption, the result of this study should not be directly reflected in decision-making without further longitudinal experimental studies. Second, only Korean women were enrolled in the present study. Since the distribution of stress and strain according to the positional relationship between the implant and proximal tibial bone geometry was analyzed, further studies targeting men[26,27] or other races[3,28] with different anatomy would be needed.

Since body weight is transmitted to the tibia through the tibial component in TKA, differences in implant characteristics can directly impact load distribution. Because cobalt-chromium alloys have a higher modulus of elasticity than Ti6Al4V alloys, stress-shielding occurs more in the surrounding bone,[12,29,30] and the thicker the baseplate the more likely bone loss will occur.[8] The shape of the component can also affect the distribution of load, which is related to the patient's anatomical geometry.[7] As these various factors work together, most clinical studies analyzing the effect of implant design have found it impossible to control for other confounders. Therefore, in many previous studies, FEA was essential to evaluate the effect of implant factors. However, since most FEA studies have used one or a small number of models, there is a limitation in that they do not reflect the anatomical diversity between patients. Therefore, we implemented FEA to control for surgical and host factors, and created 30 models to reflect the bony geometry of Koreans.

Contrary to expectations, there was no difference in the shortest distance to the anteromedial cortical bone between implants in spite of the ATC's medialized stem. This was due to the difference in stem length and sagittal angle between stem axis and baseplate (Table II). In ATC, the stem is medially biased 1.5 mm, while the distal stem tip is located proximally and anteriorly due to the short stem length and smaller sagittal angle (Figure 4a).

Therefore, although the distal stem tip of ATC was located anteromedially compared to that of the STC, there was no difference in the shortest distance, since the anteromedial cortex had an oblique orientation (Figure 4b).

When each implant was inserted, there was a difference in the ratio of load distribution to the distal stem tip and the proximal cutting plane according to the design. Compared to STC, more stress and compressive strain (minimum principal strain) were applied to the proximal medial tibial bone in patients with ATC. This result can be explained by the following reasons: first, since the medial part of the ATC baseplate has a larger area than the lateral part, a relatively larger load is transferred to the medial half of the proximal tibial bone. A second reason may be the difference in overhang rates between implants. In the 3D simulation study by Ma et al,[31] STC showed a higher overhang rate (42% to 48%) for the tibial cutting plane compared to ATC (3% to 7%) when the implant was aligned along the medial third of tibial tubercle, as in our study. Since cortical bone is stiffer than cancellous bone and bears a lot of stress,[32] more load is transferred to the cortical bone when the overhang occurs. In STC, a large load is distributed in the cortical bone of the lateral half of the proximal tibial bone, and a relatively smaller load is applied to the medial half of the cancellous bone.

As previously mentioned, ATC shows more peak stress and compressive strain in the medial proximal tibial bone, which is more advantageous in preventing stress-shielding in the relevant region.[22,23] This is contrary to the clinical study by Cho et al,[5] which showed more proximal medial tibial bone loss in ATC. It can also be explained by the following two reasons: first, this study was implemented in an experimental setting which controlled the surgical and host factors. For example, in the multiple logistic regression analysis by Cho et al,[5] when the fin of the proximal tibial stem was fitted to the medial sclerotic bone area, the odds of medial tibial bone loss were 3.79. However, since the existence of sclerotic bone was excluded in our simulation, the effect could not be analyzed. Therefore, ATC with a short stem, thin baseplate, and efficient stress distribution may show the opposite result by sclerotic bone, which will be another topic for further research. Second, there was a difference in the stress/strain change of the proximal medial tibial bone according to the distance between the distal stem tip and the anteromedial cortical bone. With ATC, as the distance decreased, the mean von Mises stress and compressive strain of the medial half of the proximal tibial bone decreased. However, with STC, the distance and mean FEA measurements of the medial half of the proximal tibial bone were not correlated. Therefore, theoretically, if the distance is decreased due to large anatomical variations (e.g. severe proximal tibial bowing or large tibial shaft offset) or surgical errors (coronal alignment or mediolateral position), ATC is more likely to be negatively affected by stress transfer to the proximal tibial bone compared to STC.

Our study had several limitations. First, since every implant has a different design, our results cannot be generalized to other products. As the specifications for each implant can differ, it is likely to result in different stress distribution. Second, this study assumed that the tibial component was composed of homogenous Ti6Al4V, but in reality the material composition ratio may slightly differ for each product. However, the difference in the composition ratio is considered to be insignificant in terms of its effect on the results. Third, since this study used models of 30 patients, experimental validations could not be performed. However, the result of our study is plausible, since FEA was conducted in a similar way to the previous FEA studies that performed experimental validation, and the measurements range was similar to those studies.[16,19] Fourth, as the analysis was conducted in a simulated experimental setting, the results may be different under in vivo conditions where host and surgical factors are involved. For example, the stress-shielding might also depend on the patient-specific bone quality around the implant. However, this was also a strength of our research. The isolated biomechanical effect of implant design on Korean women was reported for the first time. Another strength of our study is that 30 FEMs were used differently from the previous FEA studies. This enabled our study to use statistical analysis and to reflect the anatomical diversity.

In conclusion, ATC implant design, including the medialized stem and the anatomical shape of the baseplate, affects the load distribution on the periprosthetic tibial bone. Contrary to concerns previously expressed in the literature, the ATC medialized stem does not come closer to the cortical bone, and transmits more load to the medial proximal tibial bone compared to STC. However, unlike STC, the shorter the distance between the stem and the anteromedial cortical bone, the less load is applied to the medial proximal cutting plane in ATC. Therefore, when using ATC, stress-shielding should be considered in patients with severe anatomical variations, or in cases of surgical error.

References

1. **Evans JT**, **Walker RW**, **Evans JP**, **Blom AW**, **Sayers A**, **Whitehouse MR**. How long does a knee replacement last? A systematic review and meta-analysis of case series and national registry reports with more than 15 years of follow-up. *Lancet*. 2019;393(10172):655–663.
2. **Abraham R**, **Malkani AL**, **Lewis J**, **Beck D**. An anatomical study of tibial metaphyseal/diaphyseal mismatch during revision total knee arthroplasty. *J Arthroplasty*. 2007;22(2):241–244.
3. **Tang Q**, **Zhou Y**, **Yang D**, **Xu H**, **Liu Q**. The offset of the tibial shaft from the tibial plateau in Chinese people. *J Bone Joint Surg Am*. 2010;92-A(10):1981–1987.
4. **Yoo JH**, **Kang YG**, **Chang CB**, **Seong SC**, **Kim TK**. The relationship of the medially-offset stem of the tibial component to the medial tibial cortex in total knee replacements in Korean patients. *J Bone Joint Surg Br*. 2008;90-B(1):31–36.
5. **Cho BW**, **Kwon HM**, **Hong YJ**, **Park KK**, **Yang IH**, **Lee WS**. Anatomical tibial component is related to more medial tibial stress shielding after total knee arthroplasty in Korean patients. *Knee Surg Sports Traumatol Arthrosc*. 2021;29(3):710–717.
6. **Completo A**, **Talaia P**, **Fonseca F**, **Simões JA**. Relationship of design features of stemmed tibial knee prosthesis with stress shielding and end-of-stem pain. *Mater Des*. 2009;30(4):1391–1397.

7. **Scott CEH**, **Biant LC**. The role of the design of tibial components and stems in knee replacement. *J Bone Joint Surg Br*. 2012;94-B(8):1009–1015.
8. **Martin JR**, **Watts CD**, **Levy DL**, **Miner TM**, **Springer BD**, **Kim RH**. Tibial tray thickness significantly increases medial tibial bone resorption in cobalt-chromium total knee arthroplasty implants. *J Arthroplasty*. 2017;32(1):79–82.
9. **Gu S**, **Kuriyama S**, **Nakamura S**, **Nishitani K**, **Ito H**, **Matsuda S**. Underhang of the tibial component increases tibial bone resorption after total knee arthroplasty. *Knee Surg Sports Traumatol Arthrosc*. 2019;27(4):1270–1279.
10. **Kwak DK**, **Bang SH**, **Lee SJ**, **Park JH**, **Yoo JH**. Effect of stem position and length on bone-stem constructs after cementless hip arthroplasty. *Bone Joint Res*. 2021;10(4):250–258.
11. **Xie S**, **Conlisk N**, **Hamilton D**, **Scott C**, **Burnett R**, **Pankaj P**. Metaphyseal cones in revision total knee arthroplasty: the role of stems. *Bone Joint Res*. 2020;9(4):162–172.
12. **Park HJ**, **Bae TS**, **Kang SB**, **Baek HH**, **Chang MJ**, **Chang CB**. A three-dimensional finite element analysis on the effects of implant materials and designs on periprosthetic tibial bone resorption. *PLoS One*. 2021;16(2):e0246866.
13. **Zhang QH**, **Cossey A**, **Tong J**. Stress shielding in periprosthetic bone following a total knee replacement: Effects of implant material, design and alignment. *Med Eng Phys*. 2016;38(12):1481–1488.
14. **Au AG**, **James Raso V**, **Liggins AB**, **Amirfazli A**. Contribution of loading conditions and material properties to stress shielding near the tibial component of total knee replacements. *J Biomech*. 2007;40(6):1410–1416.
15. **Kimpton CI**, **Crocombe AD**, **Bradley WN**, **Gavin Huw Owen B**. Analysis of stem tip pain in revision total knee arthroplasty. *J Arthroplasty*. 2013;28(6):971–977.
16. **Cawley DT**, **Kelly N**, **Simpkin A**, **Shannon FJ**, **McGarry JP**. Full and surface tibial cementation in total knee arthroplasty: a biomechanical investigation of stress distribution and remodeling in the tibia. *Clin Biomech (Bristol, Avon)*. 2012;27(4):390–397.
17. **Morrison JB**. The mechanics of the knee joint in relation to normal walking. *J Biomech*. 1970;3(1):51–61.
18. **Kutzner I**, **Bender A**, **Dymke J**, **Duda G**, **von Roth P**, **Bergmann G**. Mediolateral force distribution at the knee joint shifts across activities and is driven by tibiofemoral alignment. *Bone Joint J*. 2017;99-B(6):779–787.
19. **Completo A**, **Rego A**, **Fonseca F**, **Ramos A**, **Relvas C**, **Simões JA**. Biomechanical evaluation of proximal tibia behaviour with the use of femoral stems in revision TKA: an in vitro and finite element analysis. *Clin Biomech (Bristol, Avon)*. 2010;25(2):159–165.
20. **Frost HM**. Wolff's Law and bone's structural adaptations to mechanical usage: an overview for clinicians. *Angle Orthod*. 1994;64(3):175–188.
21. **Pattin CA**, **Caler WE**, **Carter DR**. Cyclic mechanical property degradation during fatigue loading of cortical bone. *J Biomech*. 1996;29(1):69–79.
22. **Huiskes R**, **Weinans H**, **Grootenboer HJ**, **Dalstra M**, **Fudala B**, **Slooff TJ**. Adaptive bone-remodeling theory applied to prosthetic-design analysis. *J Biomech*. 1987;20(11–12):1135–1150.
23. **Frost HM**. A 2003 update of bone physiology and Wolff's Law for clinicians. *Angle Orthod*. 2004;74(1):3–15.
24. **Christen P**, **Ito K**, **Ellouz R**, **et al**. Bone remodelling in humans is load-driven but not lazy. *Nat Commun*. 2014;5:4855.
25. **Huiskes RIK**, **Weinans H**, **Rietbergen B**. The relationship between stress shielding and bone resorption around total hip stems and the effects of flexible materials. *Clin Orthop Relat Res*. 1992;274:124.
26. **Lim HC**, **Bae JH**, **Yoon JY**, **Kim SJ**, **Kim JG**, **Lee JM**. Gender differences of the morphology of the distal femur and proximal tibia in a Korean population. *Knee*. 2013;20(1):26–30.
27. **Cho BW**, **Nam JH**, **Koh YG**, **Min JH**, **Park KK**, **Kang KT**. Gender-based quantitative analysis of the grand piano sign in mechanically aligned total knee arthroplasty in Asians. *J Clin Med*. 2021;10(9):1969.
28. **Mohan H**, **Chhabria P**, **Bagaria V**, **Tadepalli K**, **Naik L**, **Kulkarni R**. Anthropometry of nonarthritic Asian knees: is it time for a race-specific knee implant? *Clin Orthop Surg*. 2020;12(2):158–165.
29. **Martin JR**, **Watts CD**, **Levy DL**, **Kim RH**. Medial tibial stress shielding: a limitation of cobalt chromium tibial baseplates. *J Arthroplasty*. 2017;32(2):558–562.
30. **Yoon C**, **Chang MJ**, **Chang CB**, **Song MK**, **Shin JH**, **Kang SB**. Medial tibial periprosthetic bone resorption and its effect on clinical outcomes after total knee arthroplasty: cobalt-chromium vs titanium implants. *J Arthroplasty*. 2018;33(9):2835–2842.
31. **Ma Y**, **Mizu-Uchi H**, **Okazaki K**, **et al**. Effects of tibial baseplate shape on rotational alignment in total knee arthroplasty: three-dimensional surgical simulation using osteoarthritis knees. *Arch Orthop Trauma Surg*. 2018;138(1):105–114.
32. **Osterhoff G**, **Morgan EF**, **Shefelbine SJ**, **Karim L**, **McNamara LM**, **Augat P**. Bone mechanical properties and changes with osteoporosis. *Injury*. 2016;47 Suppl 2:S11-20.

Author information:
- B. W. Cho, MD, PhD, Professor
- H. M. Kwon, MD, PhD, Professor
- W-S. Lee, MD, PhD, Professor
  Department of Orthopedic Surgery, Gangnam Severance Hospital, Yonsei University College of Medicine, Seoul, South Korea.
- K-T. Kang, PhD, Professor
- J. H. Nam, MS, Researcher
  Department of Mechanical Engineering, Yonsei University, Seoul, South Korea.
- I. H. Yang, MD, PhD, Professor
- K. K. Park, MD, PhD, Professor
  Department of Orthopedic Surgery, Severance Hospital, Yonsei University College of Medicine, Seoul, South Korea.
- Y-G. Koh, MD, Orthopaedic Surgeon, Joint Reconstruction Center, Department of Orthopaedic Surgery, Yonsei Sarang Hospital, Seoul, South Korea.

Author contributions:
- B. W. Cho: Conceptualization, Methodology, Data curation, Writing – original draft, Writing – review and editing.
- K-T. Kang: Methodology, Software, Data curation.
- H. M. Kwon: Software, Writing – original draft.
- W-S. Lee: Software, Project administration.
- I. H. Yang: Writing – review and editing, Supervision, Project administration.
- J. H. Nam: Methodology, Data curation.
- Y-G. Koh: Methodology, Data curation.
- K. K. Park: Supervision, Project administration.

Funding statement:
- The authors disclose receipt of the following financial or material support for the research, authorship, and/or publication of this article: this study was supported by a faculty research grant from Yonsei University College of Medicine.

ICMJE COI statement:
- The authors declare no competing interests.

Ethical review statement:
- This study was approved by the Severance Hospital Institutional Review Board (IRB No. 4-2020-0412). All methods were performed in accordance with the guidelines and regulations of Severance Hospital IRB. The requirement for patient consent was waived due to the retrospective nature of the study.

Open access funding
- The authors confirm that the open access fee for this article was self-funded.